45. Numerical Analysis to Predict Turning Characteristics of a Rigid Suspension Tracked Vehicle Running on a Soft Terrain

EHIME UNIVERSITY : TATSURO MURO, *TRAN DANG THAI

1-Introduction: This paper presents a numerical analysis to predict turning characteristics of a rigid suspension tracked vehicle based on a numerical method to solve set of equations written for steady stage of turning. The input to the program is the vehicle most important design characteristics and operating conditions. The basic governing equations are force and moment equilibrium equations. The set of the equations is solved for the predicted characteristics. These characteristics are forces, moment acting to the vehicle as well as other characteristics such as slip ratios, turning radius and sinkage distributions. To verify the simulation experiment on a model vehicle was carried out.

2-Equilibrium equations: Forces and moment acting to the vehicle on steady turning motion is considered as shown in Fig. 1. From the figure the equilibrium equations can be written as:

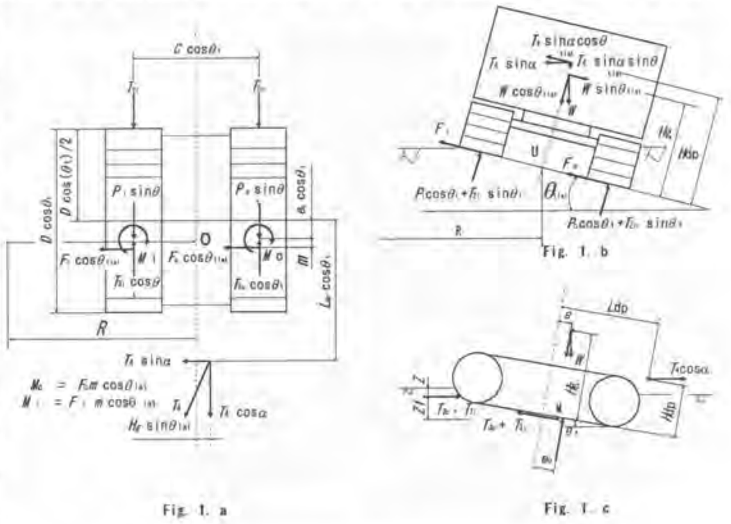

Fig. 1 Forces and moment acting to turning vehicle

$$(T_{3o}+T_{3i})\cos\theta_t - (T_{2o}+T_{2i}) - (P_o+P_i)\sin\theta_t - T_4\cos\alpha = 0 \quad (1)$$

$$W - [(P_o+P_i)\cos\theta_t + (T_{3o}+T_{3I})\sin\theta_t]\cos\theta_{tlat} - (F_o+F_i)\sin\theta_{tlat} = 0 \quad (2)$$

$$T_4\sin\alpha + (F_o+F_i)\cos\theta_{tlat} - (P_o+P_i)\cos\theta_t\sin\theta_{tlat} = 0 \quad (3)$$

$$(C/2)[(P_o-P_i)+(T_{2o}-T_{2i})\sin\theta_t] - WH_g\sin\theta_{tlat}\cos\theta_t + T_4H_{dp}\sin\alpha\cos\theta_{tlat} = 0 \quad (4)$$

$$M + (T_{20}+P_o\sin\theta_t - T_{3o}\cos\theta_t)(C/2)\cos\theta_{tlat} - (T_{2i}+P_i\sin\theta_t - T_{3i}\cos\theta_t)(C/2)\cos\theta_{tlat}$$
$$+ T_4\sin\alpha\cos\theta_t(L_{dp}-D(e_o+ei)/2) + T_4\cos\alpha H_{dp}\sin\theta_{tlat} = 0 \quad (5)$$

where T_{3o}, T_{3i} : Outer, inner thrust

T_{2o}, T_{2I}: Outer, inner rolling resistance

P_o, P_i : Outer, inner ground reaction force

T_4, α : Effective tractive effort, traction angle

F_o, F_i : Outer and inner lateral force

M, R: Turning moment, turning radius

θ_t, θ_{tlat}: Long., lateral inclination angle

W, C : Vehicle weight and track gauge

H_g: Center of gravity of vehicle H_{dp}: Height of hitch point

L_{dp}: Distance from hitch point to vehicle center of gravity D: Contact length of track

e_o, e_i: Eccentricity of ground reaction force of outer and inner track.

3- Simulation method and flowchart: For tracked vehicle with rigid suspension system the set of equations describing state of steady turning can be collapsed into the set of 5 equilibrium equations (1)-(5) with 5 independent unknowns. The independent unknowns are sinkage of front idler and rear srprocket of inner track S_{fi}, S_{ri}, lateral inclination angle θ_{tlat}, slip ratio of outer i_o (or effective tractive effort T_4) and slip ratio of inner track i_i. Other characteristics M, T_{3o}, T_{3i}, F_o, F_i, T_{2o}, T_{2i}, Po, P_i, R, S_{fo}, S_{ro}, e_o, e_i, θ_t in the set of equations can be computed from the above 5 independent unknowns. Using this approach, the problem then can be expressed as which combination of the position of the vehicle at steady turning state (specified by sinkage of front idler and rear sprocket of inner track S_{fi}, S_{ri} and lateral inclination angle θ_{tlat}) and operating conditions (specified by slip ratio of outer track i_o (or effective tractive effort T_4) and slip ratio of inner track i_i) satisfies equilibrium equations (1)-(5). The answer to this problem is to solve set of 5 equilibrium equations for 5 unknowns S_{fi}, S_{ri}, θ_{tlat}, i_o (or T4) and i_i. Newton-Raphson method for a set of nonlinear equations is used as a solving method of this set of nonlinear equations [1]. Consequently, the flow chart of the simulation is as shown in Fig.2.

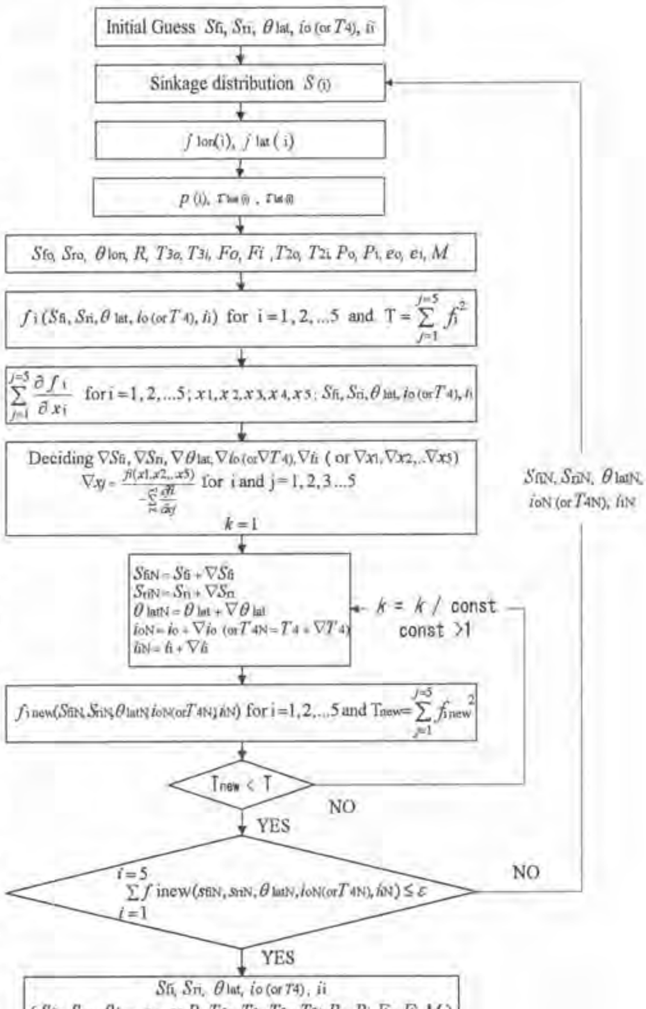

Fig. 2 Flow Chart

For a rigid suspension system the track is considered either non-extendable or extendable to a certain degree. For these cases, the sinkage distribution $S_{(i)}$ is known for the assumed vehicle position. To express sinkage distribution the track is divided into n finite sections. The sinkage distribution S(i) is then expressed as sinkages of the beginning points of each sections.

As next step distribution of longitudinal and lateral amount of slippage j_{lon}(i) and j_{lat}(i) can be computed for this guessed combination of S_{fi}, S_{ri}, θ_{tlat}, i_o (or T_4) and i_i [2].

The contact pressure distribution can then be computed by recursive solving of the following equation for each of section i of the track:

$$S_{(i)} = \left(\frac{p(i)}{k1}\right)^{\frac{1}{n1}} + S_{sl\,(i-1)} + c0\left(\frac{p(i) + p(i-1)}{2}\right)^{C1}\left[j_{(i)}^{C2} - j_{(i-1)}^{C2}\right] \qquad (6)$$

From the computed pressure distribution p(i) and distribution of longitudinal and lateral amount of slippage J_{lon}(i) and J_{lat}(i), distribution of longitudinal and lateral shear resistance τ_{lon}(i) and τ_{lat}(i) are computed using Janosi-Hanamo's equation.

Sinkage of front idler and rear sprocket of outer track S_{fo}, S_{ro}, longitudinal inclination angle θ_{lon} and turning radius R can be computed from S_{fi}, S_{ri}, θ_{tlat}, i_o and i_i using geometrical equations [2]. Longitudinal and lateral shear resistance of outer and inner track T_{30}, T_{3i}, F_o, F_i can be computed from the above calculated distribution of longitudinal and lateral shear resistance τ_{lon}(i) and τ_{lat}(i). Rolling resistance of outer and inner track T_{20}, T_{2i} are calculated from the sinkage of front idler. Resultant ground reaction force of outer and inner track P_o, P_i and their eccentricity e_o, e_i can be determined from the above calculated contact pressure distribution. Turning moment M can be determined from distribution of lateral shear resistance [2] and lateral bulldozing resistance [3].

As the next step, the values $f1$, $f2$ $f3$, $f4$, $f5$ of the left hand side of the equilibrium equations (1)-(5) are computed using the above calculated characteristics for the assumed values of S_{fi}, S_{ri}, θ_{tlat}, i_o (or T_4) and i_i.

With known values of $f1$, $f2$ $f3$, $f4$, $f5$, corrections ∇S_{fi}, ∇S_{ri}, $\nabla\theta_{tlat}$, ∇i_o (or ∇T_4) and ∇i_i can be computed by solving the set of linear equations derived from the non-linear set of equilibrium by using Taylor series as shown in the flowchart in Fig.2. The corrections are then added to guessed solutions S_{fi}, S_{ri}, θ_{tlat}, i_o (or T_4) and i_i. To assure convergence even if the guess values are far from the solutions, the newly corrected guess are checked if it reduces function T (S_{fi}, S_{ri}, θ_{tlat}, i_o (or T_4), i_i) = Σf_1^2(S_{fi}, S_{ri}, θ_{tlat}, i_o (or T_4), i_i). With these corrected guessed solution the above loop is repeated again and again until the values $f1$, $f2$ $f3$, $f4$, $f5$ of left hand side of the equilibrium equations (1)-(5) are zero (with certain tolerance). Combined with minimum finding techniques for a function T (S_{fi}, S_{ri}, θ_{tlat}, i_o (or T_4), i_i) = $\Sigma f_1^2(S_{fi}, S_{ri}, \theta_{tlat}, i_o$(or T4), i_i) as shown above the method will lead to relatively fast solutions of the equilibrium equations.

4-Simulation and experimental results: The simulation analysis and experiment were carried out for a scaled model of a bulldozer. The vehicle is turned on a loose sandy soil in a soil bin with steering ratio of 1.6 and with effective tractive effort of 0, 98.1, 147.15, 196.2 N. The traction angle was zero and the theoretical circumferencial speed of the outer track was 3.2 cm/s. Vehicle dimension and terrain-track system constants and other were shown in Table 1.

<table>
<tr><td colspan="5">Vehicle weight W (N)</td><td colspan="2">582</td></tr>
<tr><td colspan="5">Height of hitch point H_{dp} (cm)</td><td colspan="2">15</td></tr>
<tr><td colspan="5">Dist. from center of grav. to hitch point L_{dp} (cm)</td><td colspan="2">26</td></tr>
<tr><td colspan="5">Initial track tension Ho (N)</td><td colspan="2">98.1</td></tr>
<tr><td colspan="5">Height of center of gravity Hg (cm)</td><td colspan="2">15</td></tr>
<tr><td colspan="5">Contact length D (cm)</td><td colspan="2">33</td></tr>
<tr><td colspan="5">Track width B (cm)</td><td colspan="2">10</td></tr>
<tr><td colspan="5">Mean contact pressure (kPa)</td><td colspan="2">8.82</td></tr>
<tr><td colspan="5">Track gauge C (cm)</td><td colspan="2">23</td></tr>
<tr><td colspan="5">Grouser height H (cm)</td><td colspan="2">1.7</td></tr>
<tr><td colspan="5">Grouser pitch (cm)</td><td colspan="2">2.55</td></tr>
<tr><td colspan="5">Grouser thickness (cm)</td><td colspan="2">0.3</td></tr>
<tr><td colspan="5">Maximum track deflection (cm)</td><td colspan="2">1</td></tr>
<tr><td colspan="5">Radius of front idler R_f (cm)</td><td colspan="2">5.4</td></tr>
<tr><td colspan="5">Radius of rear sprocket R_r (cm)</td><td colspan="2">5.4</td></tr>
<tr><td colspan="5">Radius of road rollers R_m (cm)</td><td colspan="2">1.9</td></tr>
<tr><td colspan="5">Number of road rollers</td><td colspan="2">3</td></tr>
<tr><td colspan="5">Road roller interval (cm)</td><td colspan="2">6</td></tr>
<tr><td colspan="2">k_1 (N/cm^{n1+2})</td><td colspan="2">n_1</td><td>k_2 (N/cm^{n2+2})</td><td colspan="2">n_2</td></tr>
<tr><td colspan="2">0.278</td><td colspan="2">2.66</td><td>3.69</td><td colspan="2">0.515</td></tr>
<tr><td></td><td>m_c (N/cm^2)</td><td>m_f</td><td>a (1/cm)</td><td>c_0(cm$^{1+2c1-c2}$/N^{c1})</td><td>c_1</td><td>c_2</td></tr>
<tr><td>Lon.</td><td>0</td><td>0.738</td><td>0.141</td><td>0.386</td><td>0.573</td><td>0.601</td></tr>
<tr><td>Lat.</td><td>0</td><td>0.438</td><td>0.094</td><td>0.149</td><td>0.750</td><td>0.975</td></tr>
</table>

Table 1 Vehicle dimension and terrain-track system constants

The measured values are the sinkage of front idler and rear sprocket of the outer and inner track, radius of turning, effective tractive effort, rotary speed of each track, distance covered by both tracks, time during which the distance are covered. From the measured values the slip ratios of the outer and inner track are determined.

Fig 3 shows the comparison between measured and calculated values of sinkage of front idler of both tracks. Fig. 4 shows the same comparison but for the sinkage of rear sprocket. The figures shows good match between measured and calculated values of the sinkages. The sinkage of the inner track is observed to be smaller then that of the outer track.

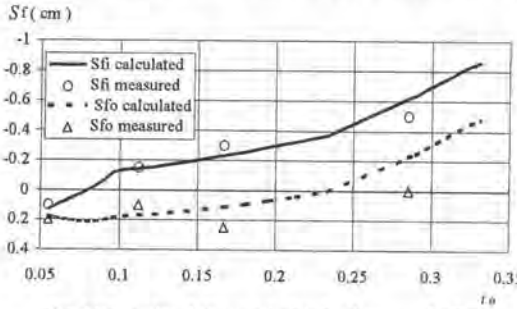

Fig. 3 Comparison between calculated and measured values of sinkage of front idler for different slip ratio of outer track i_o

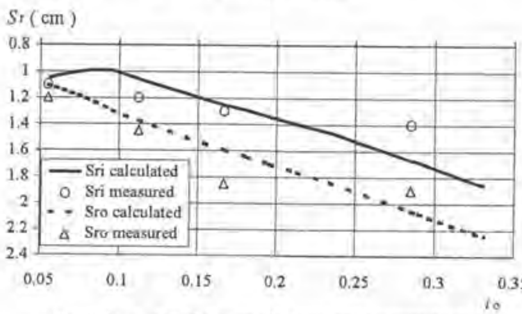

Fig. 4 Comparison between calculated and measured values of sinkage of rear sprocket for different slip ratio of outer track i_o

The comparison between the measured and calculated effective tractive effort is shown in fig. 5 while the comparison of the measured and calculated values of turning radius in fig. 6.

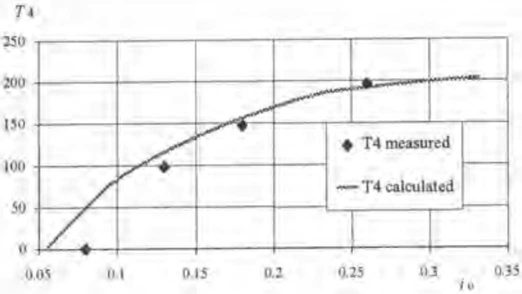

Fig. 5 Comparison between calculated and measured values of effective tractive effort T_4 for different slip ratio of outer track i_o

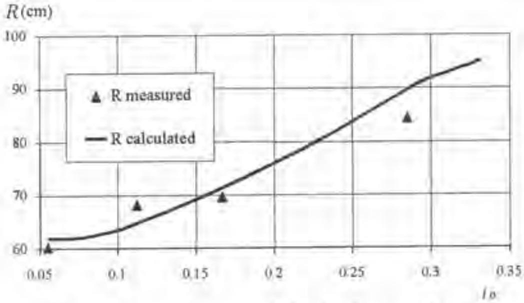

Fig. 6 Comparison between calculated and measured values of turning radius R for different slip ratio of outer track i_o

Fig. 7 to 11 shows the simulation result for 3 cases of steering ratio of 1.6, 2.2 and 3.20. The figures compare the turning characteristics of different steering ratio. Fig. 7 shows that effective tractive effort increases with the increase of slip ratio of outer track to the maximum values. The tractive effort of the smaller steering ratio is bigger than that of the larger steering ratio for the same slip ratio of outer track. Fig. 8 shows that the slip ratio of inner track increases almost linearly with the increase of steering ratio of outer track.

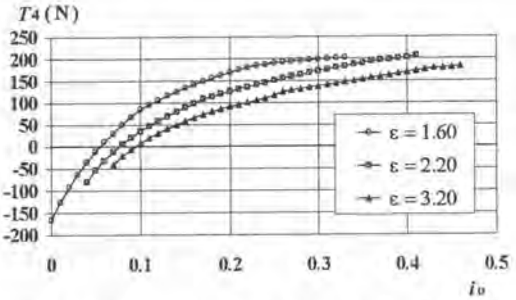

Fig. 7 Relationship between effective tractive effort T_4 and slip ratio of outer track i_o for different steering ratio

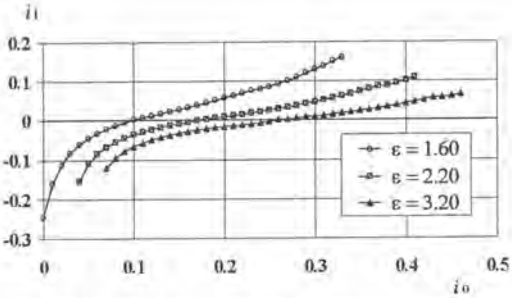

Fig. 8 Relationship between slip ratio of inner track i_i and slip ratio of outer track i_o for different steering ratio

From the fig. 9 it can be observed that there exists a minimum turning radius for all the 3 cases of steering ratio. For the same slip ratio of the outer track, the turning radius of the smaller steering ratio is bigger than that of the larger steering ratio as expected. Fig. 10 shows that the bigger the slip ratio of the outer track the smaller the turning moment can be observed. It can be explained by the fact that turning radius is bigger at the bigger slip ratio of outer track as observed in fig. 9. Fig 11 shows the contract pressure distribution for the case of steering ratio of 1.6 while the vehicle is running with slip ratio of outer track of 0.2. It is natural that the pressure shows maximum values under road rollers.

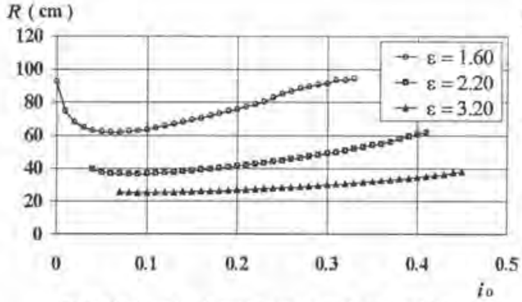

Fig. 9 Relationship between turning radius R and slip ratio of outer track i_o for different steering ratio

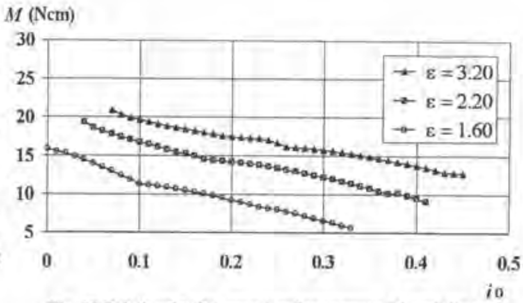

Fig. 10 Relationship between turning moment M and slip ratio of outer track i_o for different steering ratio

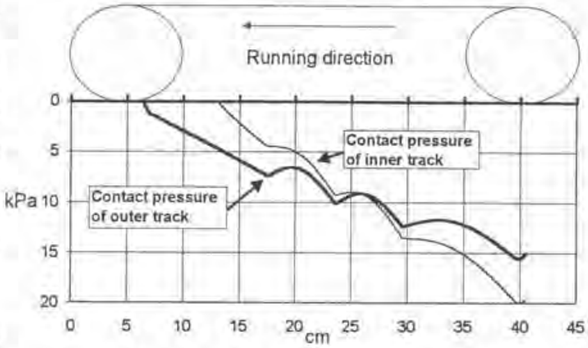

Fig. 11 Contact pressure distribution for steering ratio of 1.6 and slip ratio of outer track 0.2

5-Conclusion: The numerical analysis was established to predict turning characteristics of tracked vehicle on steady turning state and the experiment was carried to verify the simulation. From the result of the research the followings can be concluded:

1. For the case of rigid suspension system the set of equations describing steady turning state of tracked vehicle can be collapsed into the set of 5 equilibrium equations with 5 unknowns: sinkage of front idler and rear sprocket of one track, lateral inclination angle and slip ratio of outer track (or effective tractive effort) and slip ratio of inner track.
2. The numerical analysis shows that high accuracy could be observed between the calculated and measured values.
3. The sinkage of the inner track is smaller then that of the outer track for all the 3 cases of steering ratio.
4. The effective tractive effort increases with the increase of the slip ratio of outer track and is larger at smaller slip ratio for the same slip ratio of the outer track.
5. There exists the minimum turning radius in the relationship between turning radius and slip ratio of outer track.

Reference:

1. William H. Press, Saul A. Teukoisky, William T. Vetterling, Brian P. Flannery, *Numerical Recipes in C, the art of scientific computing- second edition*, Cambridge Univeristy Press, 1995, pp. 379-393.
2. Muro. T, Thai T. D, Turning Characteristics of a Bulldozer under Traction on a Weak Sandy Terrain, *Proceedings of 7th European ISTVS Conference*, 1997, 102-109.
3. E. Hegedus; A simplified method for the determination of bulldozing resistance, *LLL Report*, 1960, No. 61.